ROBOTICS

Multilegged matter transport: A framework for locomotion on noisy landscapes

Baxi Chong[1,2], Juntao He[3], Daniel Soto[3], Tianyu Wang[3], Daniel Irvine[4], Grigoriy Blekherman[4], Daniel I. Goldman[1,2,3]*

Whereas the transport of matter by wheeled vehicles or legged robots can be guaranteed in engineered landscapes such as roads or rails, locomotion prediction in complex environments such as collapsed buildings or crop fields remains challenging. Inspired by the principles of information transmission, which allow signals to be reliably transmitted over "noisy" channels, we developed a "matter-transport" framework that demonstrates that noninertial locomotion can be provably generated over noisy rugose landscapes (heterogeneities on the scale of locomotor dimensions). Experiments confirm that sufficient spatial redundancy in the form of serially connected legged robots leads to reliable transport on such terrain without requiring sensing and control. Further analogies from communication theory coupled with advances in gaits (coding) and sensor-based feedback control (error detection and correction) can lead to agile locomotion in complex terradynamic regimes.

The transport of matter across land is crucial to societies and groups (*1, 2, 3*), as well as to individuals during locomotion (*4*). Engineered self-propulsion as a means of terrestrial matter transport has been studied across scales from enormous multi-wheeled trains (Fig. 1A) to small few-wheeled and legged robots (*5–7*). For large devices, low dissipation, inertia-dominated locomotion is a commonly used matter-transport scheme. Specifically, locomotion in wheeled systems on smooth surfaces such as tracks and roads will persist over long distance unless acted on by dissipative internal or external forces (Fig. 1A).

On natural terrain, dissipation attributable to external forces can occur through interactions with terrain heterogeneities such as obstacles, gaps, or inclines (*8*), as well as through interactions with flowable materials (*9*). In dissipation-dominated applications, such as those encountered in robot movement in certain agricultural (e.g., crop fields) or confined and crowded search-and-rescue (e.g., collapsed buildings) scenarios, a system must continuously and actively generate forces and/or reduce dissipation. In part, because of our lack of understanding of the terradynamic (*9, 10*) interactions with the environments listed above, principles by which locomotors can be designed and controlled to guarantee reliable and predictable matter transport are lacking.

One engineering solution (*11*) to facilitate matter transport in complex terradynamic regimes is to use structures such as limbs to periodically make and break contact with the environment (*12*). Such dynamics can potentially simplify the thrusting interactions into a collection of discrete units, which minimize unexpected interference (*4*), thus providing an alternative to wheeled carriers on "noisy" landscapes. There have been two basic approaches of limb use in dissipation-dominated environments. The first relies heavily on sensors (*13*) to detect and respond to terrain heterogeneity in real time (*5, 14*). This approach is used for the increasingly agile locomotion in state-of-the-art legged robots (mostly bipedal or quadrupedal) (*5, 12, 14, 15*). However, the use of sensors and high bandwidth control can be expensive and restricted to specific applications.

The second approach is to instill legged robots with "mechanical intelligence" such that locomotion can be performed with minimal environmental awareness. This has been most effective with devices with more than four legs, such as hexapods (*6*) and myriapods (*16, 17*). Whereas more limbs help avoid catastrophic failures (e.g., loss of stability), terrain heterogeneity can still cause deficiencies in thrusting interactions, which substantially reduce locomotor performance (movie S1) (*18–20*). This raises the question of how variable numbers of limbs and sensors should be arranged such that one can guarantee that a locomotor can go from point A to point B in a specified time and across an arbitrarily complex landscape, and furthermore, how much sensing, feedback, bandwidth, and/or control are needed.

This question is analogous to that of information and signal transmission over noisy channels as first analyzed by Shannon nearly a century ago (*21*). Over a noiseless channel, a continuous analog signal is, in principle, able to convey an infinite amount of information (*22*). Despite its efficiency, an analog signal can be distorted by channel noise inherent in communication modalities, a property similar to heterogeneities introduced to smooth surfaces in inertia-driven matter transport (Fig. 1A). To counter channel noise in communication, Shannon (*21*) constructed a scheme in which the central idea was to digitize (encode) information into binary bit sequences and "buffer" (correct) the transmission error through redundancy (Fig. 1C).

With the analogy to information theory, it is reasonable—at least, conceptually—to anticipate reliable matter transport over noisy landscapes given sufficient redundancy of terrestrial interaction. In this work, we show that this anticipation is correct and leads to an open-loop framework for matter transport by which, for a complex terradynamic task, we can guarantee that sufficiently redundant multilegged robots can reliably and predictably self-transport over a given distance through "buffer and tolerate" dynamics without the need for sensing and feedback control or environmental awareness (Fig. 1B and movie S1) (*16*).

Development of the matter-transport framework

Our framework proceeds as follows (Fig. 2): We define a transport task as a physical entity moving to a specific destination D at a fixed time T. As shown in Fig. 2B (i), this is analogous to the intended message being transmitted across a noisy channel at a given rate. Similar to the bit-based digital signal transmission, we focus on a dissipation-dominated system in which locomotion is driven by thrusting interactions from basic active contacts (bacs, our analogy to bits), which are discrete units of active terradynamic interaction. Examples of bacs include limbs making contact with the environment (*23*) or vertical waves of contact in limbless robots (*24*). We quantify the temporal and spatial distribution of bacs as a binary sequence X^m, in which 1 denotes contact and 0 denotes noncontact [Fig. 2B (ii)]. As the locomotor implements the desired bac sequence over a noisy landscape (the analog of a noisy channel) [Fig. 2B (iii)], the terrain uncertainty can introduce contact noise to the actual bac sequence, Y^m [Fig. 2B (iv)]. This leads to a discrepancy between the actual destination $\hat{D}$ (evaluated at the scheduled time T) and the desired destination D [Fig. 2B (v)].

We next discuss our characterization and quantification of noisy landscapes. A dissipation-dominated terrain can have different types of heterogeneities, each with different complex terradynamic effects on bacs (*9*). Consider a terrain characterized by a height map, $h(x,y)$. Depending on the scale of the gradient, $[\partial h/\partial x, \partial h/\partial y]$, the terrain heterogeneity can affect the locomotion in the form of slopes, walls, or obstacles (Fig. 1B), which directly impact the thrust-generation process in the plane parallel to the terrestrial

[1]Interdisciplinary Graduate Program in Quantitative Biosciences, Georgia Institute of Technology, North Avenue, Atlanta, GA 30332, USA. [2]School of Physics, Georgia Institute of Technology, 837 State St NW, Atlanta, GA 30332, USA. [3]Institute for Robotics and Intelligent Machines, Georgia Institute of Technology, 801 Atlantic Dr NW, Atlanta, GA 30332, USA. [4]School of Mathematics, Georgia Institute of Technology, 686 Cherry St NW, Atlanta, GA 30332, USA.
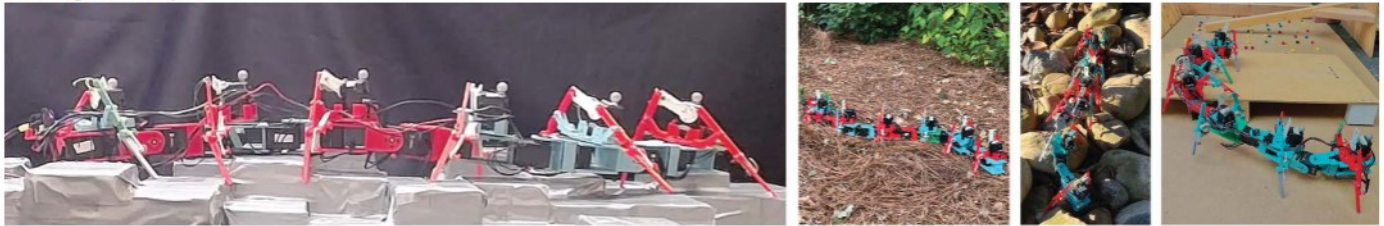*Corresponding author. Email: daniel.goldman@physics.gatech.edu
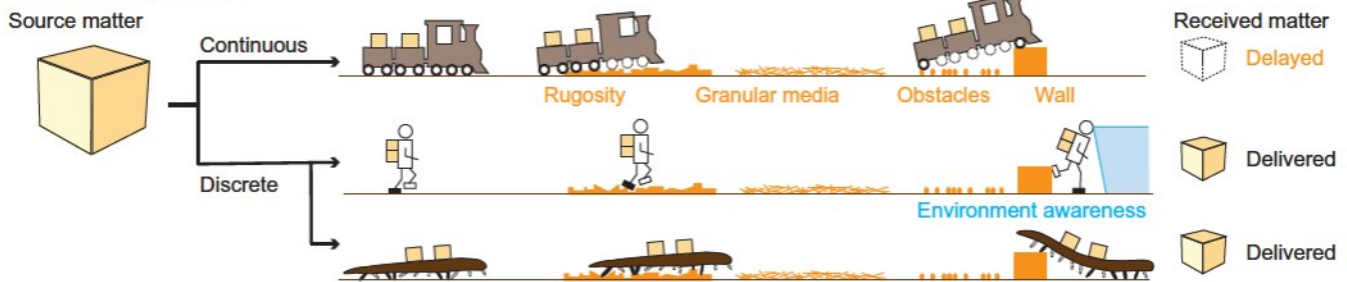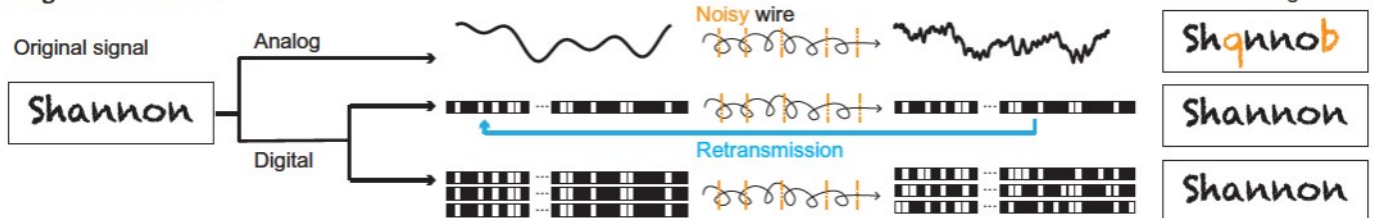
Fig. 1. Signal transmission and matter transport. (A) Matter transport with either continuous or discrete active contacts can be effective on "noise-free" tracks. Discrete redundant contacts enable effective matter transport over rugose tracks through redundancy or environmental awareness. **(B)** Multi-segmented robophysical locomotors with directionally compliant legs traverse noisy landscapes: (from left to right) a laboratory model of rugose terrain, entangled granular media, boulders, and steps. **(C)** The transmission of analog and digital signals through noisy wires. A digital signal allows reliable transmission through a noisy wire through either redundancy or a retransmission channel.

surface (e.g., a stumble) (25). Parallel thrust disturbances can be minimized by proper design of mechanical structures or passively compliant mechanisms [supplementary materials (SM), section 1.2] (16, 26). In this study, we focus on a class of noisy landscapes (rugose terrains) in which the height distribution, $h(x,y)$, can affect the supporting force distribution (e.g., missing steps) in the direction perpendicular to the terrestrial plane and therefore contaminate the intended bac sequence $(X^m \rightarrow Y^m)$.

With the notion of bacs and contact noise established, we can now model matter transport as a stochastic process. We first consider an abstract characterization of thrust generation if given one pair of legs. We quantify the instantaneous thrust over a bac, $f(t)$, as the instantaneous external force required to keep the locomotor in place at time $t \in [0,\tau]$, where τ is the duration of the bac. An example of thrust function $f(t)$ is illustrated in Fig. 3A. The nominal (undisturbed on flat terrain) average thrust is $f_n = \frac{1}{\tau}\int_0^\tau f(t)dt$.

Next, we introduce a coefficient function which encapsulates the uncertainty in the bac, $c(t)$. The terrain-disturbed thrust can be formulated by $\hat{f} = \frac{1}{\tau}\int_0^\tau c(t)f(t)dt$. We assume $c(t)$ has the property $\frac{1}{\tau}\int_0^\tau c(t) = 1$ so that the supporting force balances gravity. Further, we assume that the initiation of a bac is delayed by some time, c_1, and the duration of a bac is shortened to $\tau_u : \{c(t) = 0, t \notin [c_1, c_1 + \tau_u]\}$. Specifically, we assume c_1 to be a random variable having a uniform distribution of $c_1 \sim U(0,\tau)$, and the duration of the bac, τ_u, is assumed to be a random variable determined by the terrain rugosity. We sample τ_u from the cumulative distribution function given by $G(\tau_u) = (1 - b)\tau_u/\tau + b, \tau_u \in [0,\tau]$ so that there is a finite probability of complete bac loss, $p(\tau_u = 0) = b$, and $b < 1$ characterizes the contact noise level and offers an approximation to the rugosity of the terrain (Fig. 3C). Whenever $c_1 + \tau_u > \tau$, we extend the excessive contact duration $(c_1 + \tau_u - \tau)$ into the next bac [Fig. 2B (iii)] (SM, section 1.4). For simplicity, we assume that $c(t)$ is otherwise uniformly distributed during the bac: $\{c(t) = \tau_u^{-1}\tau, t \in [c_1, c_1 + \tau_u]\}$. In this way, the terrain-disturbed average thrust reduces to $\hat{f} = sign(\tau_u)\tau_u^{-1}f_u$, where $f_u = \int_{c_1}^{c_1+\tau_u} f(t)dt$ is the thrust disturbance. The

sign function $sign(\tau_u)$ implies that no thrust will be generated $(\hat{f} = 0)$ with complete bac loss $(\tau_u = 0)$.

As demonstrated in previous studies of dissipation-dominated multilegged locomotion on flat ground (27, 28), because of the periodic limb lifting and landing, an effective viscous (rate-dependent) cycle-averaged thrust-velocity (the average thrust and velocity over a period, respectively) relationship emerges in frictional environments, despite such thrusts being instantaneously independent of velocity. Specifically, the relationship of cycle-averaged robot locomotion velocity is derived to be linearly correlated with the cycle-averaged thrust: $\hat{v} = \gamma^{-1}\hat{f}$, where γ is the effective viscous drag coefficient (Fig. 3D). In this way, the terrain-disturbed velocity can be approximated by $\hat{v} = \gamma^{-1}sign(\tau_u)\tau_u^{-1}f_u$.

Taking the analogy from information theory in which redundant bits can bound the uncertainty from channel noise, we hypothesize that locomotors with redundant bacs can offer robustness over terrain uncertainty. A straightforward scheme to include redundancy is to decrease the transport rate by allowing more

A(i) Signal transmission

| W → Message | Encoder | X^m → Desired bits | Noisy channel | Y^m → Received bits | Decoder | $\widehat{W}$ → Estimated message |

A(ii) Locomotion

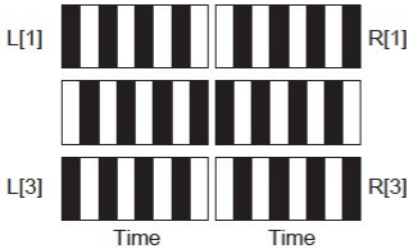| D → Mass/destination | Gait design | X^m → Desired bacs | Complex terrain | Y^m → Actual bacs | Gait realization | $\widehat{D}$ → Actual destination |
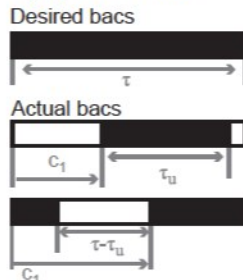
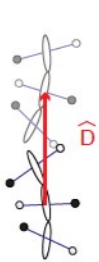**B(i)** D   **B(ii)** X^m **B(iii)** Contact noise   **B(iv)** Y^m **B(v)** $\widehat{D}$
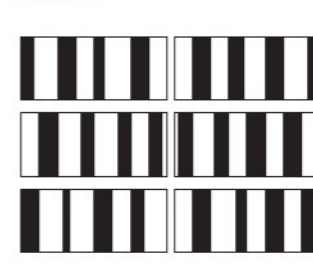
Fig. 2. Framing the matter-transport problem as a sequence of basic active contacts (bacs). (A) The correspondence of processes in **(i)** signal transmission [adapted from (*21*)] and **(ii)** locomotion (matter transport). **(B) (i)** A multilegged robot, the matter to be transported to a destination *D*. **(ii)** The desired bac sequence to reach the locomotion destination. **(iii)** Noisy landscapes can introduce contact errors such as delaying bacs and shortening the duration of bacs. We compare the desired bac (which spans a duration τ) and two terrain-contaminated bacs (each begins at c_1) with shorter duration (τ_u). **(iv)** A bac sequence contaminated by contact errors leads to a **(v)** locomotion destination $\widehat{D}$ smaller than the expected *D*.

transport time (temporal redundancy). Thus, we have:

$$\hat{v}_T^{[1]} = \frac{1}{\gamma T} \sum_{i=1}^{T} sign(\tau_u^i) \frac{f_u^i}{\tau_u^i} \quad (1)$$

where $\hat{v}_T^{[1]}$ is the average terrain-disturbed velocity over T periods, τ_u^i and f_u^i are the contact and thrust disturbance, respectively, over the ith period. Here, T represents the order of temporal redundancy. We expect the variance of the average terrain-disturbed velocity, $\sigma^2\left(\hat{v}_T^{[1]}\right)$, to decrease as T increases. Further, $\hat{v}_T^{[1]}$ converges to a Dirac delta function as T approaches infinity (proof given in the SM, proposition 3). Moreover, the expected average terrain-disturbed velocity, $\left\langle \hat{v}_T^{[1]} \right\rangle$, remains constant (by the law of large numbers).

We next evaluate the effectiveness of this temporal redundancy scheme. For simplicity, we assume D is one-dimensional, $\hat{D}_T^{[1]} = T\hat{v}_T^{[1]}$, and we note that there is no reason to expect that $\hat{D}_T^{[1]}$ should converge (to D) as T increases. Therefore, temporal redundancy can only guarantee the completion of a matter-transport task, but the exact transport duration can be indefinite.

Given the inefficiency of temporal redundancy, we develop a framework, analogous to Shannon's encoding scheme, to remove inefficient redundancy and compensate it with "redundancy of the right sort" [(*29*) p. 164] for more effective locomotion. In particular, the appropriate redundancy facilitates the simultaneous "communication" (e.g., redistribution) of bacs in response to contact noise. To develop a specific scenario for legged systems, we consider redundancy in the form of repeating serially-connected modules, in which a module is defined as a pair of legs. With proper coordination, the effect of contact noise will be shared among all bacs instead of acting on an individual bac. Because such redundancy is distributed in the spatial domain, we refer to it as spatial redundancy. Effectively, this spatial redundancy serves as a moving average filter over the contact-noise profile. For simplicity, we consider a simple module coordination that the instantaneous thrust $f(t)$ on each module is identical and invariant to the number of modules. The average terrain-disturbed velocity for N serially connected modules over T periods is:

$$\hat{v}_T^{[N]} = \frac{1}{\gamma T} \sum_{i=1}^{T} \left(sign\left(\sum_{j=1}^{N} \tau_u^{ij} \right) \frac{\sum_{j=1}^{N} f_u^{ij}}{\sum_{j=1}^{N} \tau_u^{ij}} \right) \quad (2)$$

where τ_u^{ij} and f_u^{ij} are disturbances on the jth module over the ith temporal repetition. Intuitively, in the case where there are M complete bac losses in the ith temporal repetition, $M = \left|\{j, \tau_u^{ij} = 0\}\right|$, the locomotor with N modules will essentially reduce to the configuration with $N − M$ modules. In other words, locomotors with spatial redundancy N can afford up to $N − 1$ complete bac losses without substantial thrust deficiency, which indicates that spatial redundancy can also serve to bound the uncertainty in thrust generation. We show that for fixed $T \geq 1$, $\hat{v}_T^{[N]}$ will also converge to a

Dirac delta function as spatial redundancy N approaches infinity (SM, proposition 4). The expected average terrain-disturbed velocity, $\left\langle \hat{v}_T^{[N]} \right\rangle$, can be approximated by $(1 − b^N)C_s$, where C_s is a constant determined by $f(t)$, γ, and b (SM, proposition 4). Therefore, greater spatial redundancy not only reduces variance, but also improves the expected average terrain-disturbed velocity, a feature otherwise not possible with only temporal redundancy.

For any fixed T, the distribution of actual destinations $\hat{D}_T^{[N]} = T\hat{v}_T^{[N]}$ will also converge to a Dirac delta function as N approaches infinity. Given a matter-transport task over desired distance D at scheduled time T, we consider it successful if

$$\left\| (\hat{D}, \hat{T}) − (D, T) \right\| = \left| \hat{D}_T^{[N]} − D \right| < \varepsilon \quad (3)$$

where ε is the tolerance. In this way, for arbitrary $\varepsilon > 0$ and $p_0 < 1$, there exists a finite N such that the probability of successful matter transport (subject to ε) is greater than p_0 (proof given in the SM, proposition 5). The "minimal spatial redundancy" required to achieve the probability of p_0 for tolerance $\varepsilon > 0$ is bounded by $N_{\varepsilon, p_0} \leq \frac{\log\left(1 - \frac{kD}{\sqrt[N]{p_0}}\right)}{\log(b)}$, where k is a constant that describes the locomotor speed on flat terrain, and D is the desired destination specified by distance, for one-dimensional locomotion (proof given in the SM, propositions 5 and 6).

Numerical tests of the framework

We first tested our theoretical predictions by numerical simulations. We chose a saptiotemporal

bac distribution pattern that was based on limb-stepping patterns of biological centipedes [and whose efficacy in generating locomotion in multilegged robots was previously studied in (27, 30)]. Each bac generates an instantaneous thrust given by $f(t)$, which is independent of our choice of spatial redundancy (proof given in the SM, proposition 1). We illustrate $f(t)$ in Fig. 3B. Assuming $b = 0.5$, we compared the distribution of normalized (by the nominal speed, v_{open}) terrain-disturbed velocity, v/v_{open}, for different combinations of temporal and spatial redundancy in Fig. 3E. In this example, $C_s = v_{open}$ indicates that the terrain-disturbed velocity converges to the nominal velocity (dashed black curve) given sufficient spatial redundancy.

To illustrate that spatial redundancy allows the matter-transport process (defined by the actual distance achieved, $\hat{D}$, and duration to achieve this displacement, $\hat{T}$) to converge to the desired transport-distance and duration pair (D, T), we calculate the 90% confidence interval (CI) of $\hat{D}$ as a function of T for $N = 8$ (red curves) and $N = 1$ (blue curves) (Fig. 3F). With greater spatial redundancy, the variance of $\hat{D}$ is substantially reduced, approaching the limit of nominal distance-duration relationship (dashed black curve) (Fig. 3F). Further, we numerically calculate the probability of successful matter transport (evaluated at $T = 1$) as a function of spatial redundancy N subject to different choices of tolerance ε (Fig. 3G). For all choices of ε, the success probability converges to one as N increases. Figure 3G also shows that the marginal benefit of having more legs decreases as N increases; the predicted limit is given by the dashed black curve. Finally, the locomotion performance can be affected by the terrain rugosity. We calculated N_{ε, p_0} as a function of b, the contact noise level, and plot this in Fig. 3H. We compare three combinations of ε and p_0 and notice that more rugose terrains require greater (yet finite) N_{ε, p_0}; the theoretical bound is given by the dashed black curve when $p_0 = 0.9$.

Experimental tests of the framework

Because the model assumes simplified environmental interactions, we next tested if our framework could predict locomotor performance in a physical system. We chose to work with a well-controlled laboratory multilegged robophysical model (movie S1) (design and control details are provided in the SM, sections 1.2 and 1.3), similar in design to those in (27, 30, 31). We measured the average speed and variance in such robots with different leg numbers and terrain complexity. Given that our framework indicates that matter transport can be achieved without the need for environmental awareness, we controlled all robots such that they executed their pre-
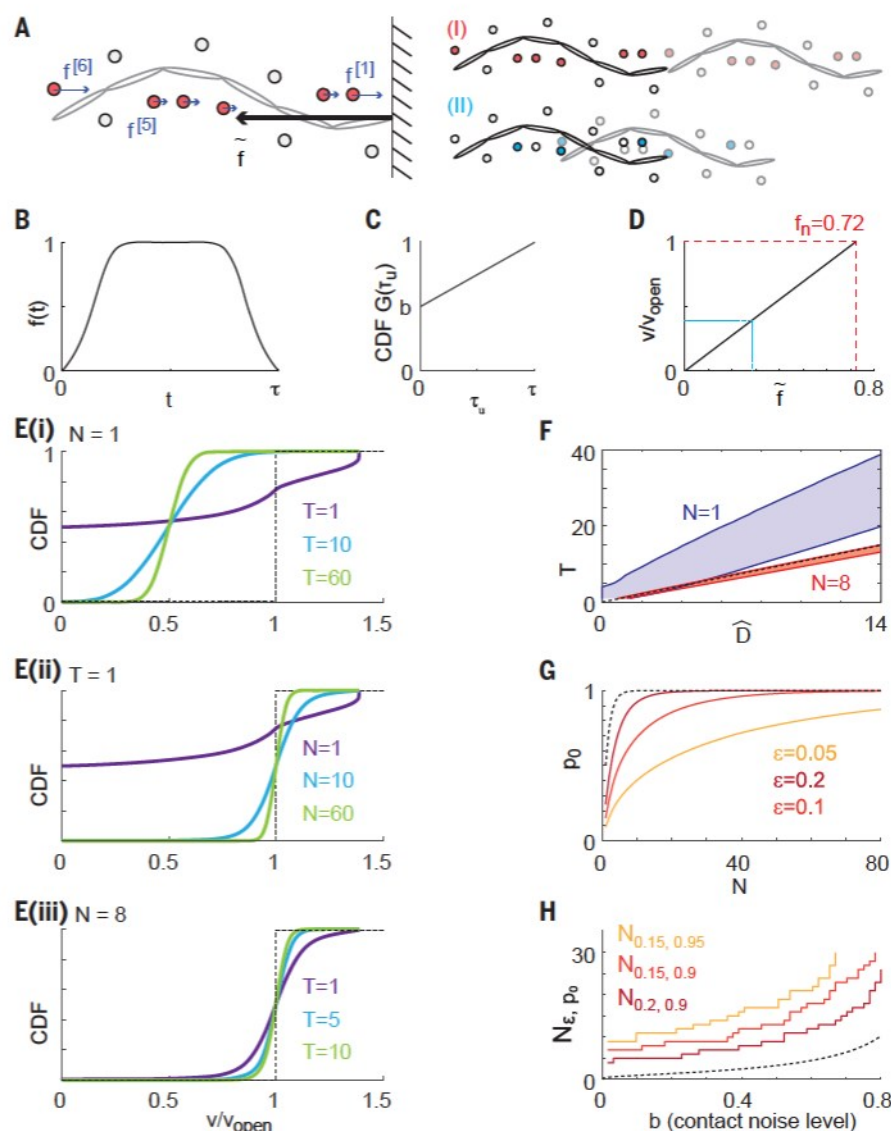

Fig. 3. Numerical simulation to test the matter-transport framework. (**A**) Illustrations of (left) thrust generation from bacs and (right) the thrust-velocity relationship. Self-propulsion with (I) nominal contact and (II) contact errors are compared. (**B**) The instantaneous thrust $f(t)$ as a function of time, derived from (28). (**C**) The cumulative distribution function (CDF) of τ_u. (**D**) The thrust-velocity (normalized by the nominal velocity) relationship. (**E**) The numerical CDF of terrain-disturbed velocity for robots with different combinations of temporal (T) and spatial (N) redundancy. (i to iii) Black dashed curves indicate the nominal CDF. (**F**) Numerically calculated 90% CI of actual destination $\hat{D}$ as a function of T. We compare two spatial redundancies: $N = 1$ (blue) and $N = 8$ (red). The nominal $\hat{D}$-T relationship is shown with the black dashed curve. (**G**) The probability of successful scheduled matter transport (p_0) as a function of spatial redundancy evaluated at different tolerance ε. We plot the theoretical predicted limit as a black dashed curve. (**H**) The relationship between N_{ε, p_0}, the minimal spatial redundancy required to achieve the desired success probability (p_0) subject to tolerance ε, and b, contact noise level. The black dashed line indicates the theoretical predicted limit when $p_0 = 0.9$.

programmed stepping patterns (open loop) and did not sense or respond to features of the environment. To facilitate comparison across different spatial redundancies N, our chosen bac sequence (the same as that in the numerical tests) has the property that, in theory, all robots share the same thrust function $f(t)$, the same performance on flat terrain, and

the same thrust-velocity relationship (proof given in the SM, proposition 2).

We constructed laboratory models of rugose terrains composed of (10×10 cm²) blocks with variation in heights (Fig. 4A). The block heights, $h(x,y)$, are randomly distributed (SM, section 1.1). Such rugose terrains ensure that limbs will experience thrust deficiency from

stochastic contact (*32*). The contact error can also arise from robot motor noise because of actuation delay, insufficient torque, or body compliance. We define the terrain rugosity, R_g, as the standard deviation of heights normalized by block side length. We tested the performance of 3-8 segmented [each segment has two directionally compliant limbs (*31*)] robophysical models on rugose terrains and recorded the bac duration (τ_u) on each leg. The distributions of τ_u measured from 225 and 309 bacs for terrain with rugosity 0.17 and 0.32, respectively, are shown in fig. S5. For $0 < \tau_u < \tau$, the measured cumulative distribution function of τ_u can be approximated by a linear function, a feature in accord with (and therefore, justifying) our assumed τ_u bac duration distribution in Fig. 3B.

We also recorded the normalized interstep average velocity (the average velocity over a step that spans the duration of a bac) of the 12-legged robot on rugose terrains during multiple steps (v/v_{open}) and compared this with the corresponding normalized bac duration (τ_u/τ) (Fig. 4B). Specifically, in each trial (five trials on each terrain), we programmed the robot to run for two periods such that there was at least one bac generated by each leg (6 legs visualizable from side-view camera). The correlation in these quantities (Fig. 4B) indicates that bac contamination is an important source of locomotor speed variability, which is in accord with our model assumption. Further, we measured the distributions of average v/v_{open} with different combinations of temporal and spatial redundancy (Fig. 4D). Specifically, we measured the average displacement (over T cycles; T is specified in Fig. 4D) of a 6-legged and a 12-legged robot on each terrain. The measured cumulative distribution functions of average v/v_{open} were in qualitative agreement with predictions from numerical tests (Fig. 3E). The sources for discrepancies between numerical and experimental tests include over-simplification of terrain characterization and contact error from robot motor noise.

As discussed earlier, for a given transport distance D, the average and the variance of transport duration are both important metrics for evaluating matter-transport performance. We measured the transport duration (in units of numbers of periods) as a function of D for a 6-legged robot and a 14-legged robot over a rugose terrain ($R_g = 0.32$). Similar to our numerical prediction in Fig. 3F, experimental results also show that spatial redundancy reduces the variance (illustrated by error bars) in transport duration (Fig. 4C). Thus, we can guarantee predictable and reliable speed on a noisy terrain during open-loop noninertial matter transport, analogous to that of the predictability of inertia-driven dynamics on noiseless (e.g., rails and roads) terrain.

To determine how spatial redundancy affects transport duration, we recorded $T_{[D=60]}$,

the time required for a robot to locomote 60 cm over rugose terrains, for robots with varying number of legs on $R_g = \{0, 0.17, 0.32\}$ (10 trials in each condition) (Fig. 4E). A hexapod can eventually self-transport 60 cm, but there is a large variance in $T_{[D=60]}$. By contrast, systems

with 16 legs can finish the self-transport task with short average time and small variance. Moreover, for systems with sufficiently high spatial redundancy (e.g., $N \geq 5$), further increases in N do not result in substantial changes in $T_{[D=60]}$, including both the average and the
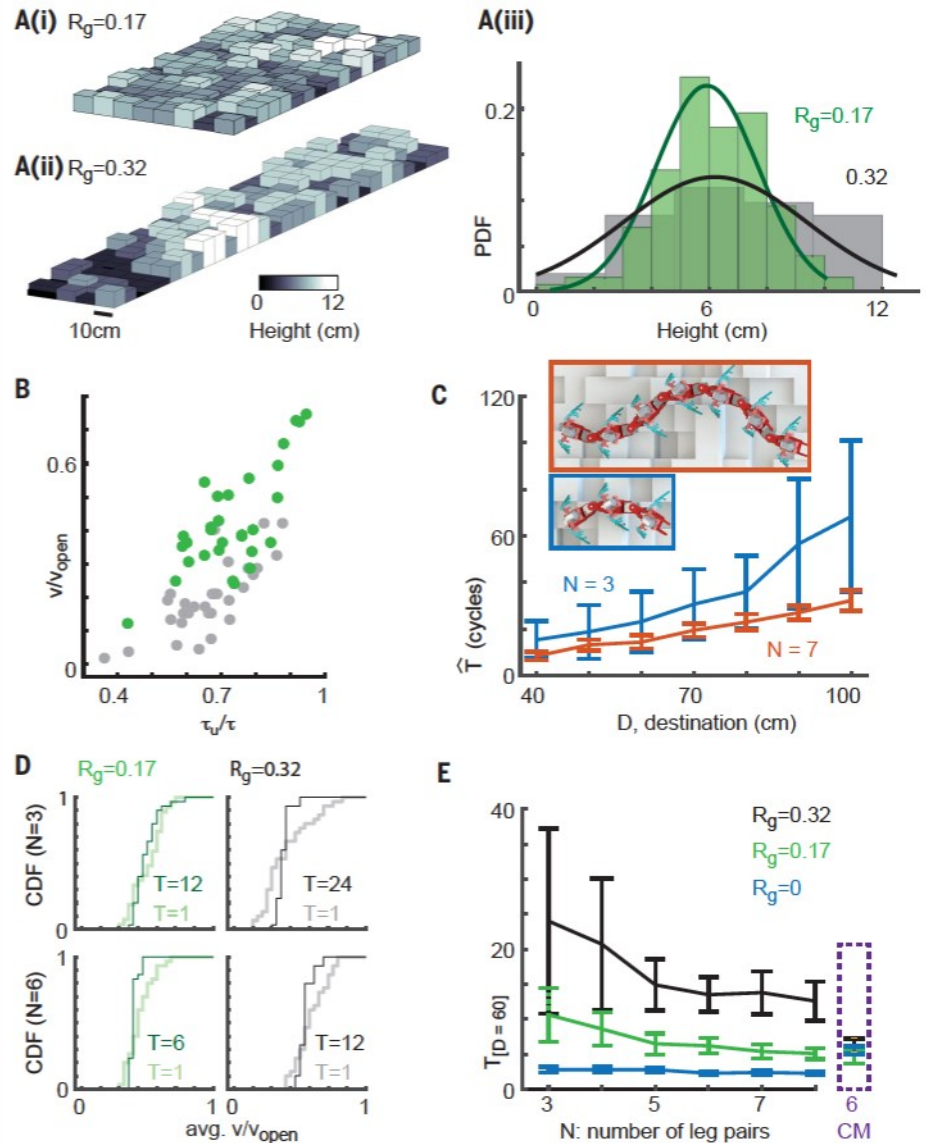

Fig. 4. Experimental test of the matter transport framework on multilegged robots. (**A**) Renderings of rugose terrains with rugosity (**i**) $R_g = 0.17$ and (**ii**) $R_g = 0.32$. The block-height distributions are shown in (**iii**). (**B**) Bac contamination leads to speed degradation in a 12-legged robot on rugose terrains. Each point denotes the robot's normalized interstep averaged velocity v/v_{open}) and a corresponding contact duration (τ_u/τ) in one bac. Color schemes are identical to those in (**A**). (**C**) The empirical transport duration ($\hat{T}$, in units of gait periods) as a function of destination distance D. We compare two robots with 14 (red) and 6 (blue) legs (renderings shown as insets). There is a large variance in transport duration for the six-legged robot, and the variance grows as destination distance increases. The 14-legged robot has a comparably tightly bounded transport duration. (**D**) The empirical distribution of average velocity on terrains with (left) $R_g = 0.17$ and (right) $R_g = 0.32$ on (Top) the six-legged robot and (Bottom) the 12-legged robot. The empirical distributions were obtained from 30 trials. (**E**) For robots with different numbers of leg pairs N, we recorded $T_{[D=60]}$, the number of periods required to transport $D = 60$ cm on terrains with (blue) $R_g = 0$, (green) $R_g = 0.17$, and (black) $R_g = 0.32$. The error bar was calculated from at least 10 trials. $T_{[D=60]}$ for contact-modulated gaits are illustrated in the dashed purple rectangle.

variance. This finding is consistent with our numerical prediction of the marginal benefit from increases in spatial redundancy after a large enough N (Fig. 3G).

From the Shannon scheme for signal transmission, it is reasonable to anticipate improved performance with more elaborate coding schemes, which we define in matter transport as designing the terradynamic interaction profile of bacs (e.g., the instantaneous thrust function $f(t)$ and thrust-velocity relationship). One straightforward method to modulate the bac-interaction profile is to change the body wave amplitude (27) or the number of waves on the body (33), which alters the temporal and spatial distribution of bacs and the associated body postures. To illustrate the potential of appropriate coding, we show one example of gait design modulation. Specifically, we imposed a head-to-tail vertical travelling wave along the body with twice the spatial frequency as the horizontal wave. This had the effect that the duration of bacs (τ) was actively and systematically shortened (contact modulation; SM, section 1.5). We tested the performance of contact-modulated (CM) multilegged robots over our rugose terrains and observed improved locomotion robustness over terrain rugosity (indicated by smaller error bars), although with some reduction of the nominal velocity v_{open} for locomotion on flat ground (Fig. 4E, dashed purple rectangle). Furthermore, with sufficient spatial redundancy ($N = 6$) as well as contact modulation, our multilegged robot was capable of traversing diverse laboratory (obstacles, inclines, and walls) environments (Fig. 1B and movie S1) and field-like environments (granular media, pebbles, and rock piles) with completely open-loop operations.

Discussion

One value of our framework lies in its codification of the benefits of redundancy, which lead to locomotor robustness over environmental contact errors without requiring sensing. This contrasts with the prevailing paradigm of contact-error prevention in the conventional sensor-based closed-loop controls that take advantage of visual, tactile, or joint-torque information from the environment to change the robot dynamics (5, 14). In this way, the complexity of matter transport can be transferred from the real-time feedback-based control (e.g., dealing with the flow of sensor information) to preprogrammed gait design. Thus, our framework could simplify matter transport tasks such as search-and-rescue (34), extraterrestrial exploration (35), or even microrobotics (36), in which robot deployments are often preferred but are challenging because of unpredictable terradynamic interactions and unreliable sensors.

However, sensory feedback can clearly be of value when a robot becomes "stuck," when terradynamic interactions vary substantially (e.g., moving from low to high rugosity terrain) or when large spatial redundancy is undesirable. In such cases, the robot must understand its state (through proprioception or exteroception) (13) and change dynamics accordingly. An analogy from information theory, error-detection coding, facilitates the augmentation of our framework with sensory-based control: in so-called error-detection coding, the presence of a "reverse channel" can facilitate the retransmission of signals, thereby improving signal transmission accuracy (21, 29). The introduction of feedback can increase the capacity of a noisy channel and can therefore decrease the coding complexity (37). We posit that a sensor-based framework in locomotion for a fixed number of bacs shares a mechanism similar to error-detection coding. If performance improvement with increased redundant bacs becomes marginal, then sensors (e.g., monitoring foot contact) that detect bac contamination could facilitate rapid environmental adaptation (e.g., whole-body gait adaptation or local leg placement adaptation) and further improve locomotion performance. Thus, a combination of redundancy-based and sensor-based mechanisms can offer unique advantages over challenging terrains, a feature similar to hybrid automatic repeat-request method (hybrid ARQ) in signal transmission (38).

In addition to the importance of locomotion in artificial locomotors, we posit that our matter-transport framework can give insights into aspects of neuromechanical and morphological evolution (39) from a physics of living systems perspective. That is, animals ranging from those which generate propulsion through a single bac-pair (i.e., bipeds) (40, 41), to those which use many bacs (i.e., myriapods) (42), are capable of traversing complex natural terrains. The importance of environmental awareness and whole-body coordination is hypothesized to diminish as the number of bacs (redundancy) increases (42–44). Thus, in biological terrestrial locomotors, there appears to be a shift toward either advanced neuromechanical control with reduced body appendages, or redundant body appendages with simplified neuromechanical control. Integration of our framework with advances in biological experimentation could yield insights into the benefits and trade-offs of diverse control architectures.

REFERENCES AND NOTES

1. J. Aguilar et al., Science 361, 672–677 (2018).
2. J. Mindell, H. Rutter, S. Watkins, Encyclopaedia of Environmental Health (Elsevier Masson, 2011), pp. 578–589.
3. H. Kreutzmann, Mod. Asian Stud. 25, 711–736 (1991).
4. R. M. Alexander, Principles of animal locomotion (Princeton Univ. Press, 2003).
5. P. Holmes, R. J. Full, D. Koditschek, J. Guckenheimer, SIAM Rev. 48, 207–304 (2006).
6. M. Raibert, K. Blankespoor, G. Nelson, R. Playter, IFAC Proceedings Volumes 41, 10822 (2008).
7. U. Saranli, M. Buehler, D. E. Koditschek, Int. J. Robot. Res. 20, 616–631 (2001).
8. M. G. Bekker, Off-the-road locomotion: Research and development in terramechanics (Univ. of Michigan Press, 1960).
9. C. Li, T. Zhang, D. I. Goldman, Science 339, 1408–1412 (2013).
10. C. Li et al., Bioinspir. Biomim. 10, 046003 (2015).
11. W. Weber, E. Weber, Mechanik der menschlichen Gehwerkzeuge (Verlag der Dietrichschen Buchhandlung, Göttingen, Germany, 1836).
12. J. Lee, J. Hwangbo, L. Wellhausen, V. Koltun, M. Hutter, Sci. Robot. 5, eabc5986 (2020).
13. J. Borenstein, H. R. Everett, L. Feng, D. Wehe, J. Robot. Syst. 14, 231–249 (1997).
14. M. Hutter et al., 2016 IEEE/RSJ international conference on intelligent robots and systems (IROS) (IEEE, 2016), pp. 38–44.
15. E. R. Westervelt, J. W. Grizzle, C. Chevallereau, J. H. Choi, B. Morris, Feedback control of dynamic bipedal robot locomotion (CRC press, 2018).
16. Y. Ozkan-Aydin, D. I. Goldman, Science Robotics 6, eabf1628 (2021).
17. S. Aoi et al., Sci. Rep. 6, 30199 (2016).
18. E. Moore, D. Campbell, F. Grimminger, M. Buehler, Proceedings 2002 IEEE International Conference on Robotics and Automation (Cat. No. 02CH37292), Washington, DC, 11 to 15 May, 2002 (IEEE, 2002), vol. 3, pp. 2222–2227.
19. C. Ordonez, J. Shill, A. Johnson, J. Clark, E. Collins, Proc SPIE Int Soc Opt Eng 8741, 240–251 (2013).
20. X. A. Wu, T. M. Huh, R. Mukherjee, M. Cutkosky, IEEE Robot. Autom. Lett. 1, 1125–1132 (2016).
21. C. E. Shannon, Bell Syst. Tech. J. 27, 379–423 (1948).
22. A. Feinstein, IEEE Trans. Inf. Theory 4, 2– 22 (1954).
23. R. J. Full, D. E. Koditschek, J. Exp. Biol. 202, 3325–3332 (1999).
24. H. C. Astley et al., Proc. Natl. Acad. Sci. U.S.A. 112, 6200–6205 (2015).
25. H. Forssberg, J. Neurophysiol. 42, 936–953 (1979).
26. P. E. Schiebel et al., Robophysical modeling of bilaterally activated and soft limbless locomotors, Biomimetic and Biohybrid Systems: 9th International Conference, Living Machines, Freiburg, Germany, 28 to 30 July, 2020 (Springer International Publishing, 2020), pp. 300–311.
27. B. Chong et al., Proc. Natl. Acad. Sci. U.S.A. 120, e2213698120 (2023).
28. D. Zhao, B. Bittner, G. Clifton, N. Gravish, S. Revzen, Proc. Natl. Acad. Sci. U.S.A. 119, e2113222119 (2022).
29. J. R. Pierce, An Introduction to Information Theory: Symbols, Signals and Noise (Courier Corporation, 2012).
30. B. Chong et al., Bioinspir. Biomim. 17, 046015 (2022).
31. Y. Ozkan-Aydin, B. Chong, E. Aydin, D. I. Goldman, 2020 3rd IEEE International Conference on Soft Robotics (RoboSoft), New Haven, CT, USA, 15 May to 15 July, 2020 (IEEE, 2020), pp. 156–163.
32. A. Jacoff, A. Downs, A. Virts, E. Messina, Proceedings of the 8th Workshop on Performance Metrics for Intelligent Systems, Gaithersburg, MD, USA, 19 to 21 August, 2008 (NIST, 2008), pp. 29–34.
33. B. Chong et al., Int. J. Robot. Res. 40, 1547–1562 (2021).
34. J. Whitman, N. Zevallos, M. Travers, H. Choset, 2018 IEEE International Symposium on Safety, Security, and Rescue rRobotics (SSRR), Philadelphia, PA, USA, 6 to 8 August, 2018 (IEEE, 2018), pp. 1–6.
35. N. D. Naclerio et al., Sci. Robot. 6, eabe2922 (2021).
36. J. J. Abbott, Z. Nagy, F. Beyeler, B. J. Nelson, IEEE Robot. Autom. Mag. 14, 92–103 (2007).
37. S. Tatikonda, S. Mitter, IEEE Trans. Inf. Theory 55, 323–349 (2008).
38. C. Lott, O. Milenkovic, E. Soljanin, 2007 IEEE Information Theory Workshop on Information Theory for Wireless Networks, Bergen, Norway, 1 to 7 July, 2007 (IEEE, 2007), pp. 1–5.
39. B. Chong, T. Wang, E. Erickson, P. J. Bergmann, D. I. Goldman, Proc. Natl. Acad. Sci. U.S.A. 119, e2118456119 (2022).
40. D. S. Marigold, Exerc. Sport Sci. Rev. 36, 145–151 (2008).
41. T. Krasovsky, A. Lamontagne, A. G. Feldman, M. F. Levin, Gait Posture 39, 378–385 (2014).
42. K. Diaz, E. Erickson, B. Chong, D. Soto, D. I. Goldman, J. Exp. Biol. 226, jeb244688 (2023).
43. S. Sponberg, R. J. Full, J. Exp. Biol. 211, 433–446 (2008).
44. B. Bläsing, H. Cruse, J. Comp. Physiol. A Neuroethol. Sens. Neural Behav. Physiol. 190, 173–183 (2004).

45. D. Soto, B. Chong, Code for rugose terrain generation, Zenodo (2021); https://doi.org/10.5281/zenodo.7121219

Multilegged matter transport: A framework for locomotion on noisy landscapes

Baxi Chong, Juntao He, Daniel Soto, Tianyu Wang, Daniel Irvine, Grigoriy Blekherman, and Daniel I. Goldman

Editor's summary
Locomotion over rugged terrain, whether human or robotic, generally requires extensive feedback to allow for adjustments in stride to compensate for cracks, inclines, or changes in surface composition. This ability typically requires a network of sensors to detect changes in terrain. Chong *et al.* show that an alternative approach requiring minimal environmental awareness can guarantee a successful arrival using information theory. The authors draw a parallel between having multiple, connected legs on the robot and having signal transmission protocols that minimize error in transmission—in this case, the "signal" being transmitted is the body of the robot. —Marc S. Lavine

View the article online
https://www.science.org/doi/10.1126/science.ade4985
Permissions
https://www.science.org/help/reprints-and-permissions

Use of this article is subject to the Terms of service